J. Electrochem. Sci. Eng. **12(5)** (2022) 989-1000; http://dx.doi.org/10.5599/jese.1120

Open Access : : ISSN 1847-9286
www.jESE-online.org

Original scientific paper

Spray pyrolisis deposition and characterization of Cd-TiO_2 thin film for photocatalytic and photovoltaic applications

Masilamani Raja Sekaran[1,2], Parasuraman Kumaresan[1,2,✉], Subramanian Nithiyanantham[3,✉], Vatakkaputhanmadom Krishnaiyer Subramanian[4] and Sundar Kalpana[5]

[1]*PG & Research Department of Physics, Thiru A. Govindasamy Govt. Arts College, Tindivanam 604002, India*
[2]*Department of Physics, Research and Development Centre, Bharathiar University, Coimbatore 641046, India*
[3]*PG & Research Department of Physics, (Ultrasonics, NDT and Bio-Physics Divisions), Thiru, Vi. Kalyanasundaram Govt. Arts and Science College, Thiruvarur 610003, India*
[4]*PG & Research Department of Chemistry, Periyar Govt. Arts College, Cuddalore 607001, India*
[5]*PG & Research Department of Physics, AMET University, Chennai 603112, India*

Corresponding author: ✉s_nithu59@rediffmail.com, ✉lokeshkumaresan@yahoo.com

Received: September 28, 2021; Accepted: June 17, 2022; Published: August 15, 2022

Abstract

In the present paper, an innovative approach to enhance the photocatalytic efficiency and energy of photovoltaics by modifying the surface morphology of a TiO_2 is demonstrated.The photovoltaic device provides sustainable power efficiency in TiO_2 (TO) and Cd-TiO_2 (CTO) thin films grown through spray pyrolysis. The structural and optical properties of the prepared undoped and Cd doped TiO_2 thin films were studied. The morphology and content of the produced samples were studied using scanning electron microscopy (SEM with EDAX). A UV-Vis spectrophotometer was used to record the optical absorption spectra of TiO_2 nanoparticles. XRD analysis showed that TO and CTO had anatase structure, and the average crystalline size was calculated as 132.0 nm.The photocatalytic efficiency of TO and CTO for degradation of Rodhamine B (RhB) dye was examined. Also, power-voltage (P-V) and photocurrent-voltage (I-V) output current intensity relations were discussed.

Keywords

Energy materials; doped TiO_2 thin film; photocatalytic degradation; photocurrent-voltage characteristics

Introduction

Among materials useful for either photocatalysis orphotovoltaic devices, TiO_2 has been immensely inquired due to its photochemical corrosion, strong optical absorption, nontoxicity, and

favorable band edge positions [1-3]. TiO_2 is a common n-type semiconductor with a direct bandgap with large chemical stability. TiO_2 is a biosafe and biocompatible material that can be used in a wide range of applications, including photovoltaics, photocatalysis, and optical, biomedical and other purposes.

The photovoltaic and photocatalytic performances of nanocrystalline TiO_2 depend on several parameters, such as morphology, crystalline phase and single crystallinity [2,3]. Therefore, intense research has usually focused on fabricating one-dimensional TiO_2 nanostructures having morphologies with size-related optical and electrical properties. TiO_2 properties depend greatly upon its existing phase, *i.e*. anatase, rutile or brookite. The anatase phase shows an indirect optical band gap of 3.2 eV, while the rutile phase has a direct band gap of 3.06 eV. It absorbs in the UV regime of solar radiation (less than 5 %), which significantly limits its widespread applications [4-9]. To expand light absorption to the visible region, doping with transition metals has usually been employed. Among all transition metals used for TiO_2 doping, Cd is the most favored due to large solid solubility [10,11].

Photocatalysis is a valuable method for wastewater treatment, particularly in the textile industry. The textile industry wastewater produced in each of the processes like the sizing of textile fibers, bleaching, calendering, dyeing and finishing has high pH and temperature, which along with a large amount of oil and grease sodium substances create problems in the treatment and disposal [12]. Azo dyes and metal-phthalocyanines are the most common synthetic colorants (60–70 %) used to dye natural textile fibers, which results in dyes and heavy metals found in the by-products. The degradation of azo dyes and removal of heavy metals were found insufficient by the application of conventional aerobic processes and other physical-chemical techniques usually used for the treatment of wastewater.The photocatalysisis is often applied with other advanced techniques [13,14], showing much better results.

In the present work, we focus on titania with dopant Cd, and titania free from dopant, for optical and other related properties [15-17].

Experimental

Titanyl acetylacetonate ($C_{10}H_{14}O_5Ti$) and cadmium nitrate ($Cd(NO_3)_2$) were supplied by Aladdin Regent Company. Hydrochloric (HCl) ethanol solution was purchased from Sino Pharm Chemical Reagent Co., Ltd. The natural dye Hibiscus rosiness flower extract (anthocyanins) and other materials were high purity. Deionized water was used throughout the work.

Cd doped TiO_2 thin films were coated on microscopic glass substrates (FTO) using spray pyrolysis. For making deposition, $C_{10}H_{14}O_5Ti$ and $Cd(NO_3)_2$ were used as the titanium and dopant sources, respectively. In order to prepare TiO_2 thin film, the FTO substrate was cleaned for 15 min with prepared solutions. While performing this experiment, the FTO substrate was put firmly over the heating plate ~24 cm from the sprayer. The sample holder's top surface was maintained at a constant temperature of about 80 ^oC, and the rotational speed was about 100 r/min. Before making deposition, the substrate was pre-heated for a specific time, and then the solution was sprayed over the microscopic glass substrate having the dimension of 75×25 mm^2 at the temperature of 500 ^oC (T_s=500 ^oC). Finally, the grown film was harvested through a regular process. In the photocatalyst tests, 5 mg of nanocomposite of TO and CTO were dissolved in 100 ml of deionized water containing 0.025 M of TO and CTO, respectively. After mixing, the solution was maintained in a dark environment before being exposed to visible light.

The structural characterization of the deposited film was confirmed by X-ray diffraction equipped with (SHIMADZU-6000) monochromatic Cu-Kα radiation ,λ = 15.406 nm.The XRD patterns were

recorded in 2θ intervals from 10 to 90° with the steps of 0.05° at room temperature. The surface morphology was examined through HR-SEM (JEOL-JES-1600). Elementary dispersive X-ray (EDX) evaluation experiments were performed on an FEI Quanta FEG 200 instrument with an EDX analyzer facility at 25 °C. High-resolution transmission electron microscopy (HR-TEM) images were taken using a JEOL-JEM-2010 UHR instrument operated at an acceleration voltage of 200 kV with a lattice image resolution of 0.14 nm. Photoluminescence (PL) spectra at room temperature were recorded using a Perkin-Elmer LS 55 fluorescence spectrometer.UV spectral measurements were done using a Hitachi-U-2001 spectrometer. The absorbance spectrum is observed by unity subtracting the transmission and reflectances, measured by a spectrophotometer (HORIBA, iHR320) equipped with an integrating sphere and commercial detectors. The photovoltaic properties of the material were characterized by recording the photocurrent-voltage (*I-V*) curve under the illumination of AM1.5 (100MW/cm^2).

Further, the photocatalytic phenomenon, UV light allow to expose on the deposited films. When the catalyst is lit with energy equivalent to or more than the band gap value, organic molecules are destroyed. After being exposed to UV radiation, the color of dye solutions degraded noticeably due to the presence of a catalyst.

Results and discussion

HR-SEM and EDX analysis

In order to understand the physical nature of the prepared surface, a morphological study of CTO thin films was examined. Morphologyof Cd doped TiO_2 exhibits uniform and compact distribution of spherical grains. HR-SEM image presented in Figure 1(a) shows a nano spherical shaped structure and highly porous nature, as can be viewed clearly through the clusters formed during the growth. In Figure 1(b), the EDX spectrum shows the presence of Cd and O in CTO thin film that is free from any impurity.

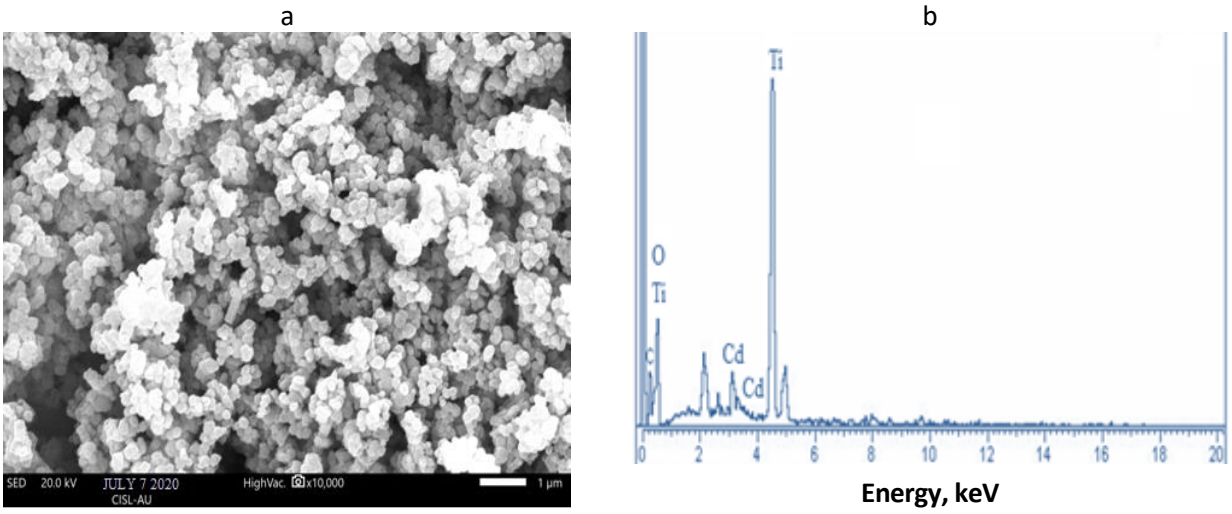

***Figure 1**. (a) SEM image and (b) EDS analysis of Cd TiO_2 (CTO) film*

HR-TEM analysis

HR-TEM image presented in Figure 2(a) shows a cross-sectional view of Cd doped TiO_2 thin film. The film thickness is estimated to be around 20 nm, and a clear spherical shaped structure is shown in Figure 2a. In Figures 2b and 2c, typical average particle size range distribution of 24.2 to 138.2 nm was identified. In Figure 2d,the 3D structure of the selected cross-section is highlighted**.**

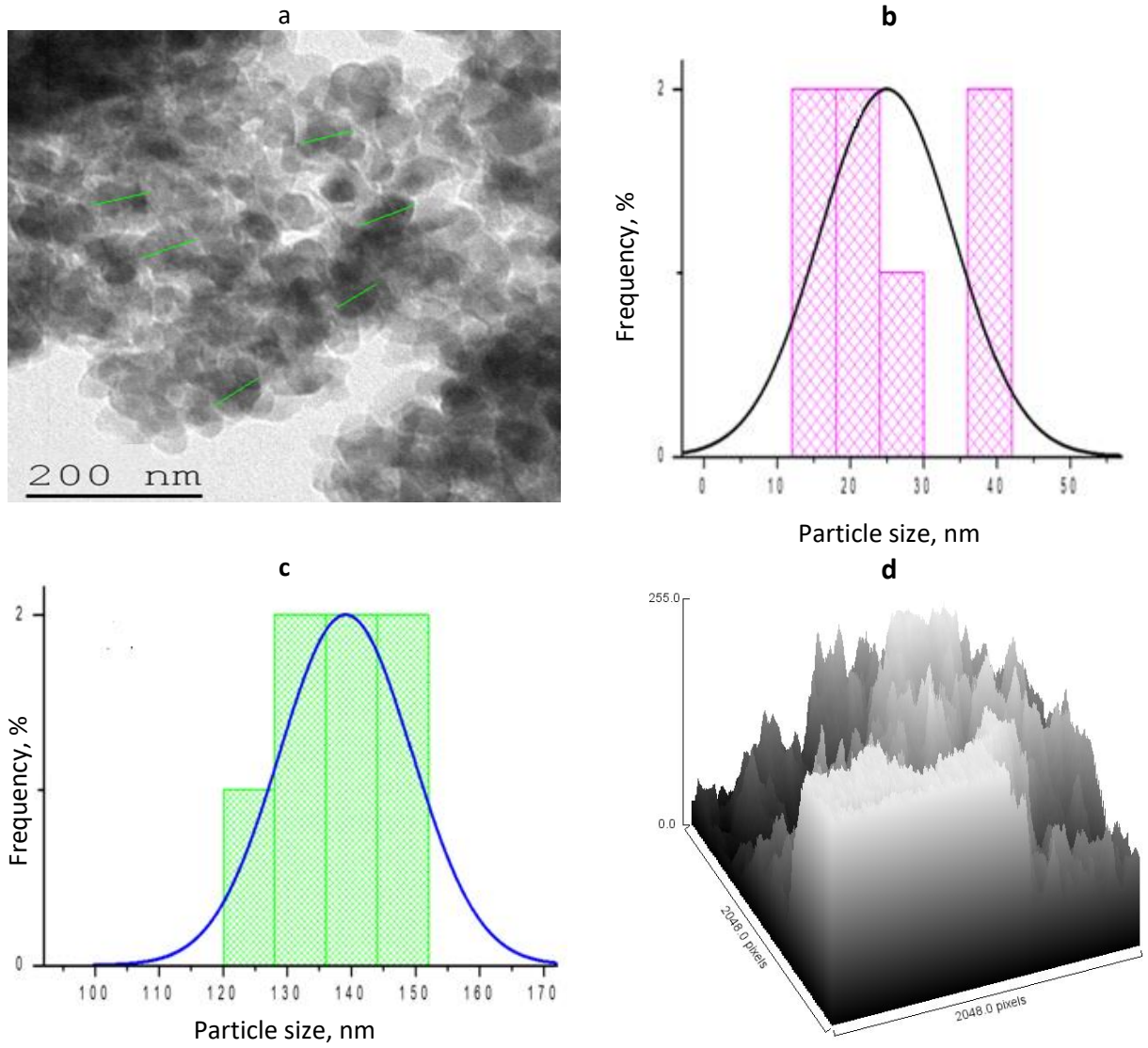

Figure 2. *(a) HR-TEM micrograph, (b-c) average particle size (24.2 to 138.2 nm) and (d) image profile 3D structure of CTO thin film*

Structural characterization

To recognize the crystal structure, an X-ray diffraction study was accomplished using XRD patterns of CTO thin film shown in Figure 3. It is revealed that CTO thin film belongs to the hexagonal wurtzite structure having sharp peaks representing high crystallinity structure at 25.25, 34.62, 37.57, 48.5, 54.0, 63.0 and 69.12 and 75.0º characteristic for (101), (004), (200), (105) and (204) planes. The average crystalline size (*D*) of the prepared material was estimated through Scherrer's formula:

$$D = K\lambda / \beta \cos\theta \quad (1)$$

where β is full width half maximum, θ is diffraction angle, λ is the wavelength of X-rays used, and *K* is the constant. The average crystalline size of Cd doped TiO_2 particles was found to be 16 and 14 nm, respectively, confirming thus nano-sized particles.

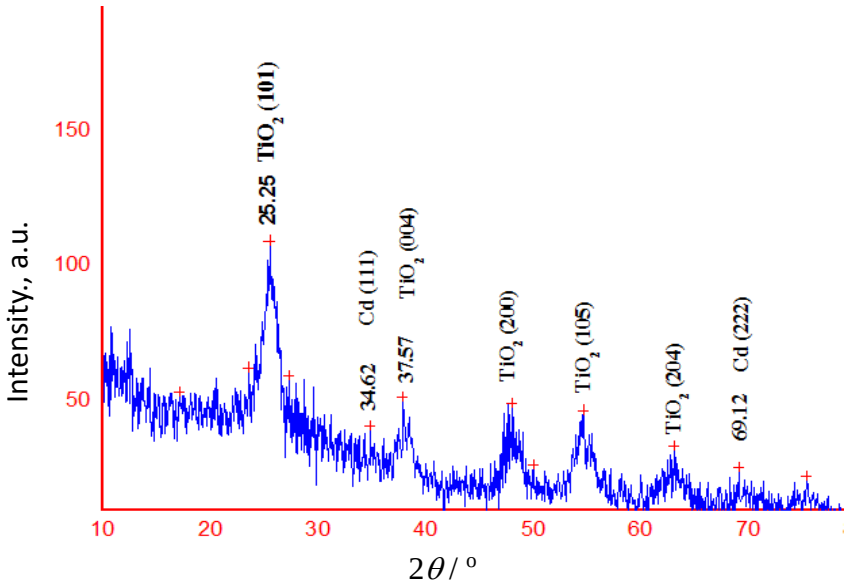

***Figure 3**. XRD analysis of CTO thin film*

Optical properties

The optical absorption properties of TO and CTO allow for analyzing the results of UV-visible spectroscopy, which are shown in Figure 4.The optical absorption of TO and CTO thin films for small changes in absorption edge towards the maximum wavelength was observed. The increasing dispersion and gradual decreasing nature of extinction coefficient (*k*) is attributed to increasing doping concentration. With increasing impurities in the host material, the doped CTO film shows a decrease in wavelength region due to high absorption radiation. The basic absorption edge was observed in both UV and visible regions by absorption in a range around 200-800 nm.

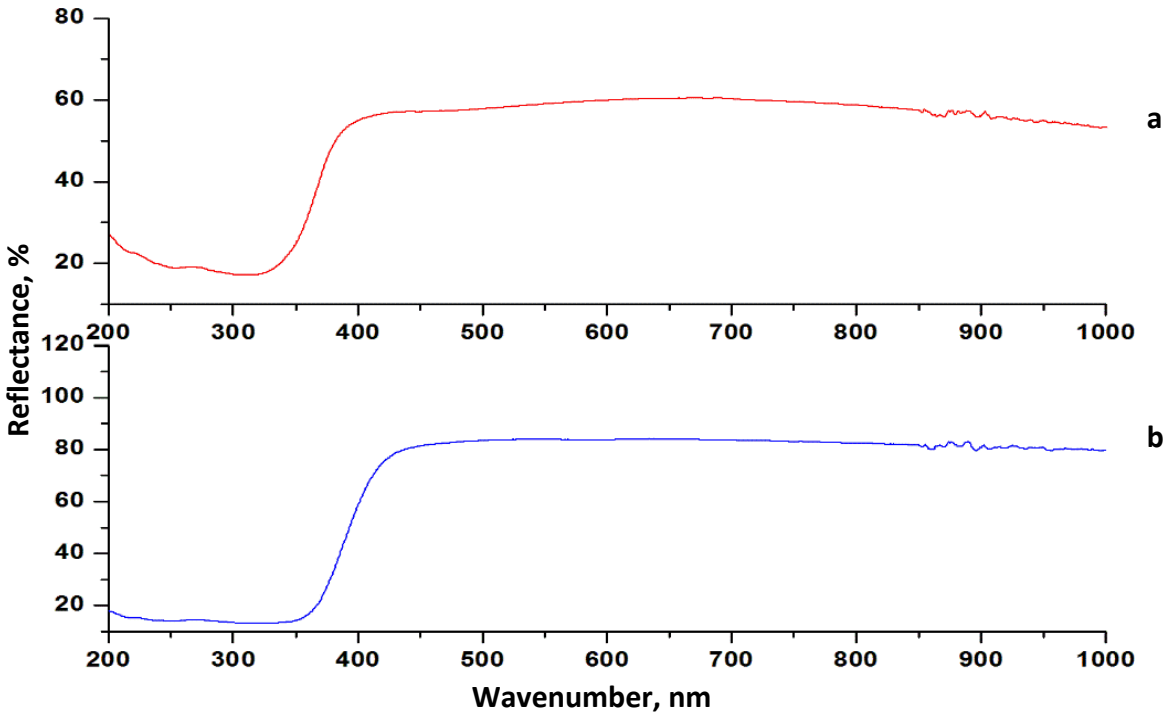

***Figure 4**. Optical study of (a) CTO and (b) TO thin films*

The optical energy band gap of both materials was calculated using the Tauc plot. The extrapolation of this curve indicates the optical band gap value, *i.e.* suitability for photovoltaic

applications [18]. The band gap efficiency of TO and CTO thin films is shown in Figure 5. The band gaps of TO and CTO thin films were found to be 3.2 and 2.8 eV, respectively, revealing that the band gap decreases with Cd content, leading to higher photo-electro catalytic efficiency.

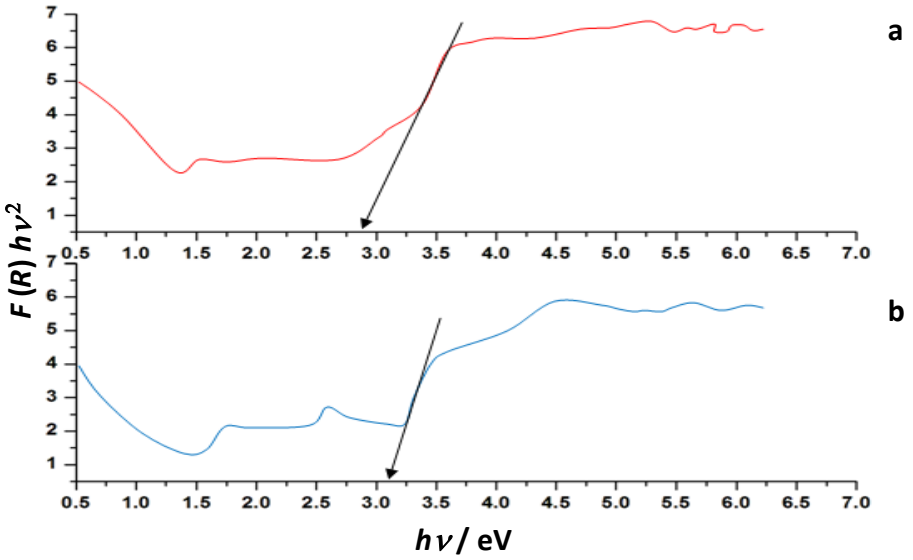

Figure 5. *Optical study of band gap energy of (a) TO and (b) CTO thin films*

Photoluminescence (PL) analysis

Figure 6 illustrates typical photoluminescence (PL) spectra of prepared TO and CTO thin films. PL spectra show emission peaks in the range 350–500 nm. However, no change in excitation and emission peak has been noted due to the increasing size of the quantum confinement effect.

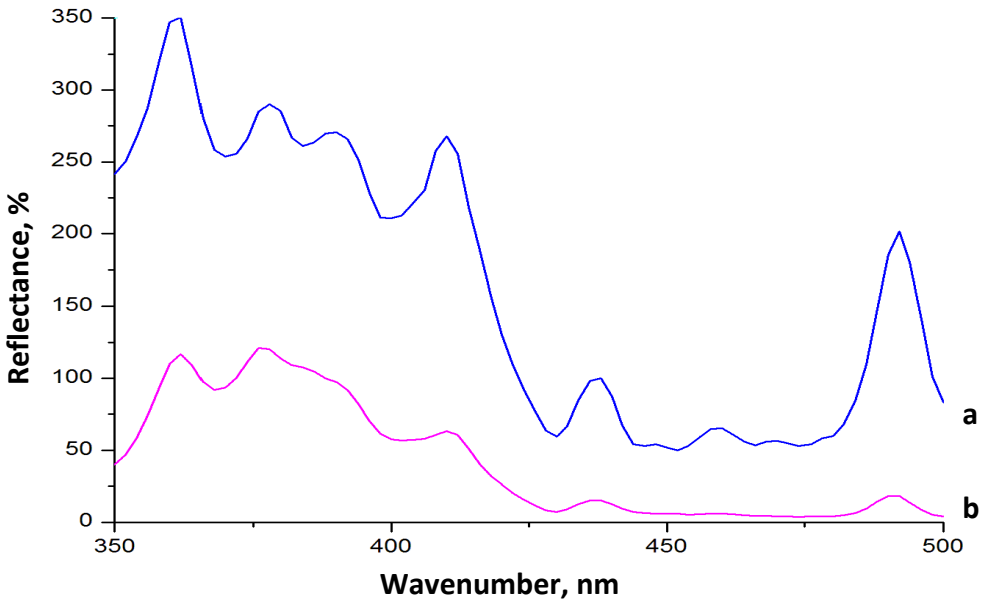

Figure 6*. PL analysis of (a) TO and (b) CTO thin films*

This research shows that oxygen ions significantly modify synthesized CTO thin films' optical characteristics. The luminous intensity of TO and CTO thin film nanoparticles was observed at max = 360 nm. The recombination of free carriers, charge trapping, and photogenerated electrons and holes in a semiconductor caused the photon energy band gap to decrease from 3.2 to 2.8 eV for doped thin film photons, indicating that visible luminescence is produced due to structural defects emissions at 375-490 nm appear blue-green band edge and oxygen vacancy (green emission

at 500 to 540 nm). The results show that the lower reflectance of CTO thin films improved photo-electro applications [19-21].

Photocatalytic efficiency forRhB degradation with UV-light

The manufactured TO and CTO thin films and Rhodamine B (RhB) dye (0.1 mM) in an aqueous solution were subjected to UV light. Organic compounds are degraded by light when the catalyst is illuminated with energy equal to, orhigherthan the band gap value. The color of dye solutions devalued notably under the existence of catalyst after its exposure to UV light. Photocatalytic efficiency of TO and CTO thin films was found to be remarkable under UV light as shown in Figure 7.

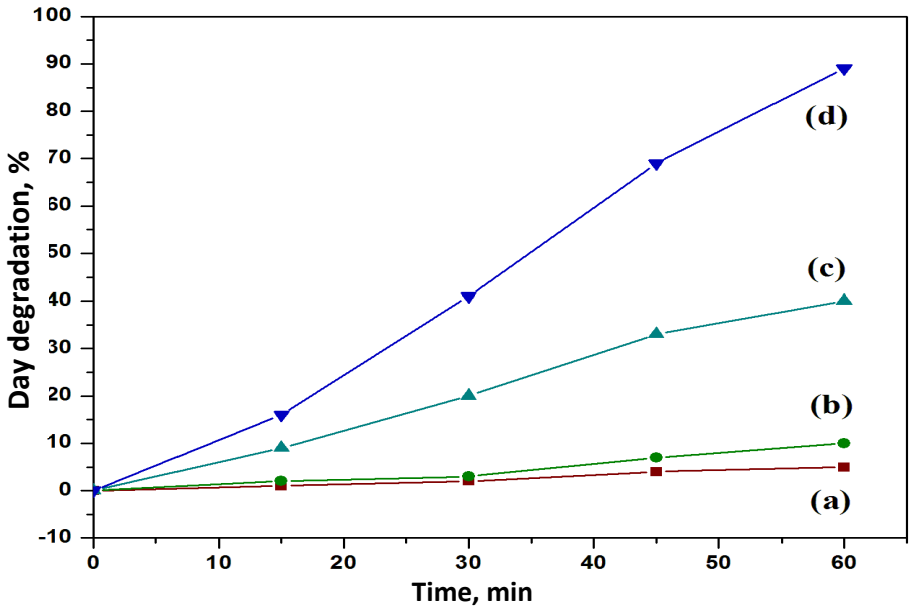

Figure 7. *Photocatalytic efficiency of RhB dye degradation under UV-light irradiation:(a) dye + UV; (b) dye+CTO+dark; (c) dye + TO + UV; (d) dye + CTO + UV*

Such remarkable efficiency clearly indicates the transfer of photoexcited electrons from the conduction band of the semiconductors to the empty electron levels of the dye. The existence of metal prevents the recombination process in a semiconductor and thus intensifies photocatalytic reactions. A graph plotted in Figure 7 represents the dye removal against the irradiation time to determine the optimal irradiation time for eliminating RhB dye molecules. It can be noted that the maximum removal efficiency of RhB occurs at 60 min, and after this time, RhB adsorption remains unchanged. Therefore, 60 min irradiation time has been considered the ideal value for further studies. Similarly, after 60 min irradiation time, the CTO composite decolorized the dye solutions remarkably, exhibiting enhanced photocatalytic activity compared to clear TO thin film. The photodegradation of dye with 60 min showed higher efficiency of doped CTO thin film compared to undoped TO thin film. The results indicate following content of degradation:dye + UV at 0-60 min (0, 1, 2, 4 and 5 %), dye + Cd-TiO_2 at 0 to 60 min (0, 2, 3, 7 and 10 %), dye + TiO_2 + UV at 0 to 60 min (0, 9, 20, 33 and 40 %) and dye + Cd-TiO_2+ UV in 0 to 60 min (0, 16, 41, 69 and 89 %).

Photocatalytic activity (reusability)

To confirm the strength of the CTO catalyst, five cycles of photocatalytic tests were carried out and the results are depicted in Figure 8. The stability and reusability of TO and CTO thin films were investigated by repeating the cycle (1 to 5) of the degradation experiment.

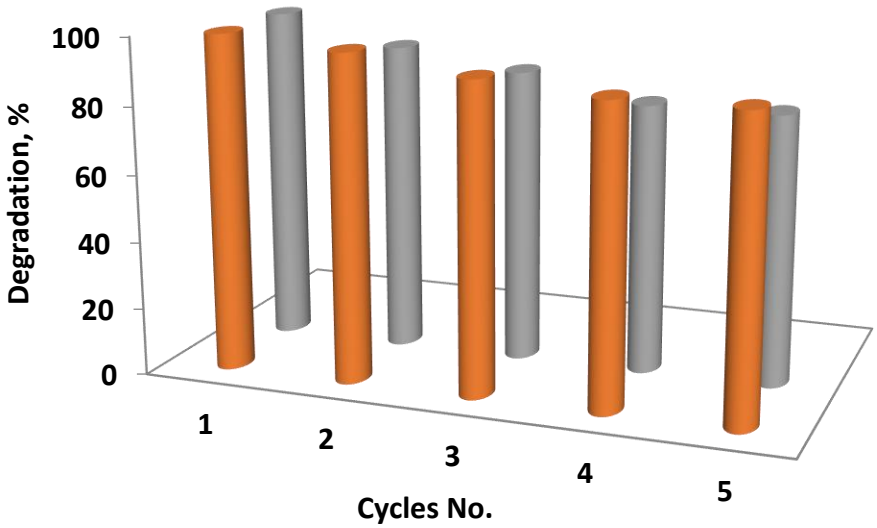

Figure 8. *Stability and reusability of* (■) *TO and* (■) *CTO thin films*

Figure 8 shows that the 1st to 3rdcycles resulted in different levels of degradation, whereas the 4th and 5th cycles resulted in almost equal degradation. During 1st-5th cycles, the undoped TO exhibited 100, 92, 87, 80 and 80 % degradation, while for Cd doped CTO thin film, 100, 97, 92, 89 and 89 % degradation was recorded. Based on the analysis of all parameters, it was concluded that Cd doped TiO_2 thin films exhibit more effective dye degradation compared to TO thin films. The first three cycles have shown almost no loss in degradation efficiency and obtained minute loss after the fourth cycle, verifying its steady nature [21].

Photocatalytic efficiency (mechanism)

The mechanism of photocatalytic degradation of RhB dye over CTO is defined by eqs. (2) to (7):

^{1}RhB $dye_0 + h\nu \rightarrow {}^1$RhB dye_1 (2)

^{1}RhBdye_1 + ISC $\rightarrow {}^3$RhB dye_1 (3)

Cd-TiO_2 (SC) + $h\nu \rightarrow e^-$(CB) + h^+(VB) (4)

$OH^- + h^+ \rightarrow {}^\bullet OH$ (5)

$^\bullet OH + {}^3$RhB $dye_1 \rightarrow$ LeucoRhB dye (6)

LeucoRhB dye → Product (7)

where, SC is a semiconductor, CB is a conduction band, VB is a valance band and h^+ is an electron hole, respectively. The main aim of this part of the study was to assess the catalyst activity for the degradation reaction of RhB dye. RhB forms an energized singlet state as it absorbs radiation of the preferred wavelength. In addition, it experiences interfacial surface complex (ISC) to give its triplet state. During excitation, the transition of an electron in the Cd-TiO_2 thin film semiconductor utilizes this energy. An electron can be absorbed from OH^- by a hole (h^+) in the semiconductor valence band, resulting in hydroxyl radicals, $^\bullet OH$. RhB dye will be oxidized by this hydroxyl radical, which may eventually breakdown into products. The role of OH as an active oxidizing species in the degradation of RhB dye was confirmed, and the rate of degradation was significantly slowed in the presence of an OH scavenger [22,23]. The scheme of organic dye degradation at the TiO_2 surface under UV-light irradiation is shown in Scheme 1.

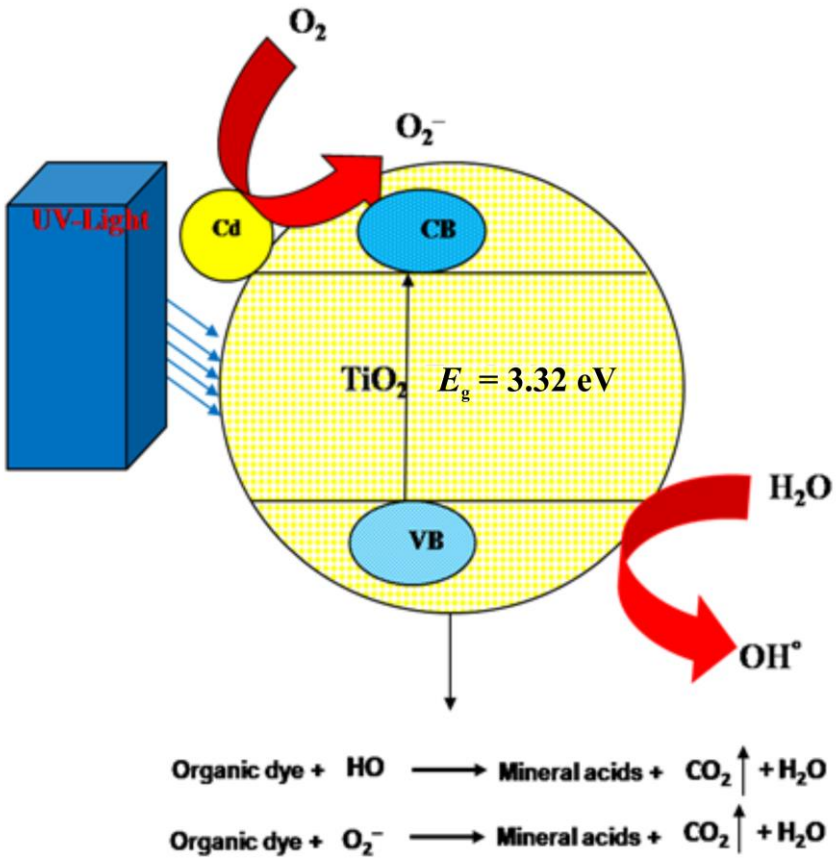

Scheme 1. Mechanism of organic dye degradation at TiO_2 surface under UV-light irradiation

I-V characterization

The efficiency of conversion from solar energy to electrical energy for TO and CTO thin films in dye-sensitized solar cells (DSSC) was measured from the short-circuit current (J_{sc}) at open circuit photovoltage (V_{oc}). Figure 9 shows current density–voltage curves for natural dyeing with Rosa[b] flower extract (anthocyanins) based DSSC. The strong dye absorbance was identified at 516 nm for TO and CTO thin films. The solar power efficiency of TO [J_{sc} = 5.4 mA/cm^2] thin film is less when it is compared to CTO thin film [J_{sc} = 6.3 mA/cm^2] [24-26].

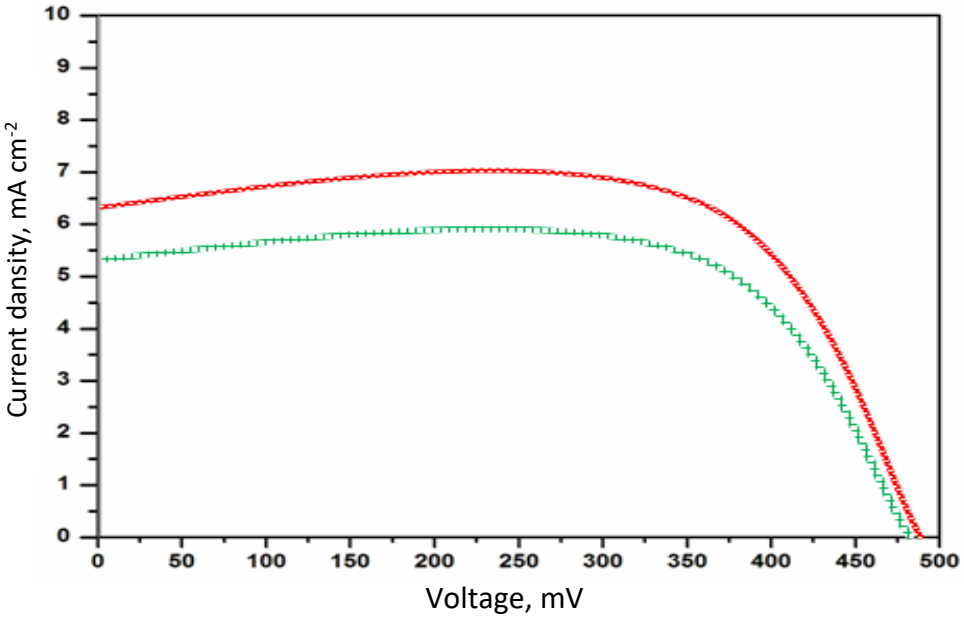

***Figure 9**. I-V characterization of (—) TO and (—) CTO thin films on GCE in 0.1 M KCl (dye-coated substrate)*

P-V characterization

With the same procedure, the solar power efficiency of TO (J_{sc} = 75.0 mA/cm^2) thin film is less compared to CTO thin film (J_{sc} = 80.0 mA/cm^2)(Figure10).

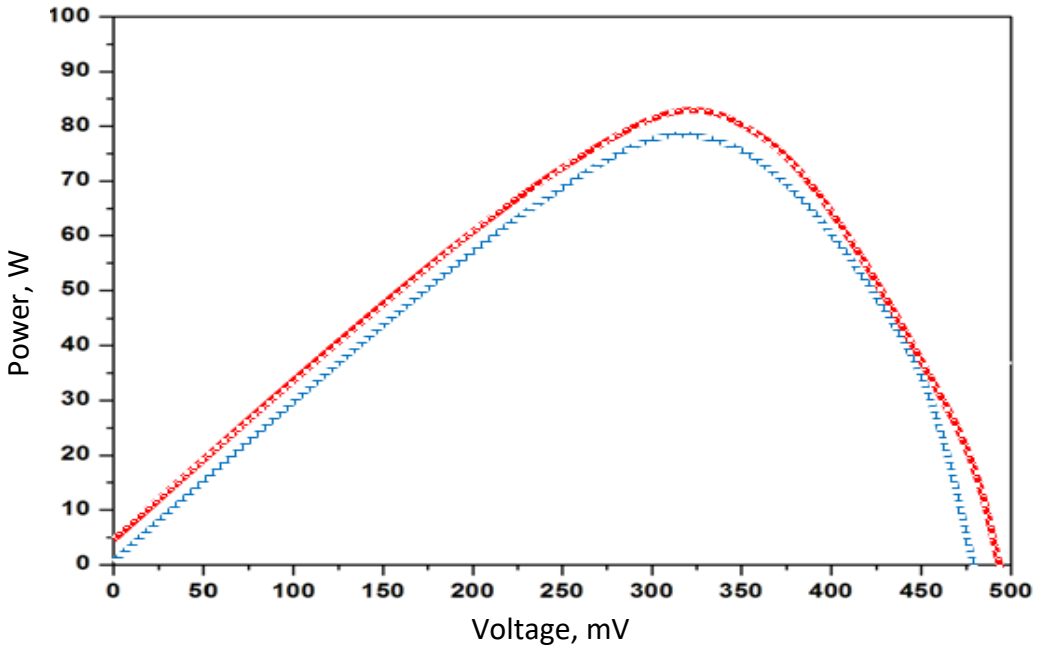

***Figure 10**. P-V characterization of* (—)*TO and* (—) *CTO thin film on GCE in 0.1 M KCl (dye coated substrate)*

Conclusion

In summary, TiO_2 (TO) and Cd-doped TiO_2 (CTO) thin films were synthesized by spray pyrolysis technique, their photovoltaic properties and photocatalytic degradation activity were examined. The investigated samples have an anatase phase and a size of about 138.2 nm, which confirms formation of nanoparticles. The band gap value for TiO_2 (TO) and Cd doped TiO_2 (CTO) thin films decreased from 3.2 to 2.8 eV. The surface morphology of films showed nano-spherical shaped structure, while crystalline nature was confirmed by EDX analysis. Photocatalytic efficiency of CTO for RhB dyedegradation showed a higher value than the undoped thin TO film. The stability and reusability of TO and CTO thin films were investigated by repeating degradation cycles. According to the findings, the addition of a blocking layer at the interface of FTO and Cd doped TiO_2 thin film layer enhanced the *P-V* and *I-V* output suitable for electrochemical industrial applications.

Acknowledgement:*The authors are grateful to acknowledge The Principal, TAG Govt arts College, Tindivanam, for providing the necessary facility to complete this work.*

References

[1] P. Roy, S. Berger, P. Schmuki, *Angewandte Chemie International Edition* **50(13)** (2011) 2904-2939.https://doi.org/10.1002/anie.201001374

[2] M. Xu, P. Da, H. Wu, D. Zhao, G. Zheng, *Nano Letters* **12(3)** (2012)1503-1508. https://doi.org/10.1021/nl2042968

[3] J. Yin, Y. Huang, S. Hameed, R. Zhou, L. Xie, Y. Ying, *Nanoscale* **12(34)** (2020) 17571-17589. https://doi.org/10.1039/D0NR04156D

[4] S. Hoang, S. Guo, N. T. Hahn, A. J. Bard, C. B. Mullins, *Nano Letters* **12(1)** (2012) 26-32. https://doi.org/10.1021/nl2028188

[5] Q. Huaulmé, V. M. Mwalukuku, D. Joly, J. Liotier, Y. Kervella, P. Maldivi, S. Narbey, F. Oswald, A. J. Riquelme, J. A. Anta, R. Demadrille, *Nature Energy* **5** (2020) 468-477. https://doi.org/10.1038/s41560- 020-0624-7
[6] J. A. Kumar, K. D. Kumar, H.-J. Kim, *Electrochimica Acta* **330** (2020) 135261. https://doi.org/10.1016/j.electacta.2019.135261
[7] M. V. Khenkin, E. A. Katz, A. Abate, *et al., Nature Energy* **5** (2020) 35-49. https://doi.org/10.1038/s41560-019-0529-5
[8] M. Aftabuzzaman, C. Lu, H. K. Kim, *Nanoscale* **12(34)** (2020) 17590-17648. https://doi.org/10.1039/D0NR04112B
[9] N. N. Ilkhechi, A. R. Aghjehkohal, E. F. Tanour Aghaj, M. Mozammel, *Journal of Materials Science: Materials in Electronics* **28** (2017) 4598-4605. https://doi.org/10.1007/s10854-016-6097-6
[10] Y. A. Kumar, S. Sambasivam, S. A. Siva, K. Zeb, W. Uddin, T. N. V. Krishna, K. D. Kumar, I. M. Obaidat, K.-J. Kim, *Electrochimica Acta* **334** (2020) 137318. https://doi.org/10.1016/j.electacta.2020.137318
[11] H. Aydin, *Journal of Physical Chemistry and Functional Materials* **2(1)** (2019) 18-22. https://dergipark.org.tr/tr/download/article-file/768305
[12] L. Tian, X. Zhang, X. Xu, Z. Pang, X. Li, W. Wu, B. Liu, *Dyes and Pigments* **174** (2020) 108036. https://doi.org/10.1016/j.dyepig.2019.108036
[13] K. Ahmad, Q. M. Suhail, *Multi-junction Polymer Solar Cell,* in: *Handbook of Nanomaterials and Nanocomposites for Energy and Environmental Applications,* O. V. Kharissova, L. M. Torres-Martínez, B. I. Kharissov, Eds., *Springer, Cham*, 2021 pp**.** 1817-1833. http://doi.org/10.1007/978-3-030-36268-3_196
[14] A. Arunkumar, S. Shanavas, R. Acevedo, P. M. Anbarasan, *Structural Chemistry* **31** (2020) 1029-1042. https://doi.org/10.1007/s11224-019-01484-w
[15] Q. Qiao, Y. Xie, J. T. McLeskey, *Journal of Physical Chemistry C* **112(26)** (2008) 9912-9916. https://doi.org/10.1021/jp7115615
[16] X. Nie, S. Yin, W. Duan, Z. Zhao, L. Li, Z. Zhang, *Nano* **16(01)** (2021) 2130002. https://doi.org/10.1142/S1793292021300024
[17] M. Murugalakshmi, M. Anitha, A. C. Dhanemozhi**,** *Materials Today*: *Proceedings* **8(1)** (2019) 357-361. https://doi.org/10.1016/j.matpr.2019.02.123.
[18] B. Ergin,E. Ketenci, F. Atay, *International Journal of Hydrogen Energy* **34(12)** (2009) 5249-5254. https://doi.org/10.1016/j.ijhydene.2008.09.108
[19] B. Subash, B. Krishnakumar, M. Swaminathan, M. Shanthi, *Langmuir* **29(3)** (2013) 939-949. https://doi.org/10.1021/la303842c
[20] N. Mariotti, M. Bonomo, L. Fagiolari, N. Barbero, C. Gerbaldi, F. Bella, C. Barolo, *Green Chemistry* **22(21)** (2020) 7168-7218. https://doi.org/10.1039/D0GC01148G
[21] S. Balachandran, R. Karthikeyan,K. Selvakumar, M. Swaminathan, *International Journal of Environmental Analytical Chemistry* (2020). https://doi.org/10.1080/03067319.2020.1790541
[22] T. Delgado-Montiel, J. Baldenebro-López, R. Soto-Rojo, D. Glossman-Mitnik, *Molecules* **25(16)** (2020) 3670. https://doi.org/10.3390/molecules25163670
[23] M. R. Pallavolu, Y. A. Kumar, G. Mani, R. A. Alshgari, M. Ouladsmane, S. W. Joo, *Journal of Electroanalytical Chemistry* **899** (2021) 115695. https://doi.org/10.1016/j.jelechem.2021.115695
[24] I. F. Elegbeleye, N. E.Maluta, R. R.Maphanga, *Molecules* **26(4)** (2021) 955. https://doi.org/10.3390/molecules/26040955

[25] Y. A. Sumanth, R. A. Sujatha, S. Mahalakshmi, P. C. Karthika, S. Nithiyanantham, S. Saravanan, M. Azagiri, *Journal of Materials Science: Materialsin Electronics* **27** (2016)1616-1621. https://doi.org/10.1007/s10854-015-3932-0

[26] C. Dragonetti, A. Colombo, *Molecules* **26(9)** (2021) 2461. https://doi.org/10.3390/molecules26092461